VELOCITY TO POROSITY TRANSFORM IN MARINE SEDIMENTS

MANIKA PRASAD AND JACK DVORKIN
DEPARTMENT OF GEOPHYSICS, STANFORD UNIVERSITY
STANFORD, CA 94305-2215

ABSTRACT

We apply a new effective medium model for calculating elastic moduli of high-porosity ocean-bottom sediments to several Ocean Drilling Program (ODP) well log data sets from offshore Amazon delta, Peru margin, and Bengal Bay. The model relates the bulk and shear elastic moduli of the sediment to porosity, differential pressure, elastic constants of the grains, and pore-fluid compressibility. As a result, we can accurately match sonic well log data using porosity and differential pressure as main input. Therefore, velocity data can be used to infer porosity and pressure.

INTRODUCTION

Velocity to porosity transforms are an important component of in well log data analysis and interpretation. The traditional transform recommended by many handbooks and manuals is Wyllie's time average equation (Wyllie et al., 1956). This equation states that the travel time of an elastic wave in rock is simply the sum of the travel times through the solid and pore-fluid components of the rock. Although, Wyllie's time average equation has an appearance of a first-principle-based relation, it is strictly empirical, as was emphasized by the authors of the relation. Moreover, the experimental basis for this equation includes consolidated rocks and, therefore, this transform should not be unconditionally applied to unconsolidated sediments (Dvorkin and Nur, 1998). This is especially true for the shallow marine environment.

A first-principle model that relates velocity to porosity does exist for marine sediments that are in a state of suspension, i.e., they do not have any frame stiffness. This is the Wood model (Wood, 1941) where the effective bulk modulus of the sediment is the iso-stress (Reuss, 1929) average of the solid and fluid phase bulk moduli, and the shear modulus is zero. However, shear waves can propagate in marine sediments below the mudline (e.g., Hamilton, 1976), which indicates that the dry frame of these sediments has non-zero shear rigidity and that the sediments are not in suspension.

Recognizing this fact, researchers have developed a number of empirical site-specific equations for calculating the elastic-wave speeds in marine sediments versus depth, porosity, and differential pressure (e.g., Hamilton, 1971 and 1976; Richardson and Briggs, 1993). Wilkens et al. (1992) used Wood's model in combination with actual P-wave velocity measurements to estimate the shear modulus and shear-wave velocity in marine sediments.

A different class of models adds "free" fitting parameters to existing functional forms (such as Wyllie's time average equation). For example, Nobes et al. (1986) combined Wood's equation and Wyllie's time average to arrive at an ad-hoc weighted equation. Lee et al. (1996) also used multi-phase weighted equations (based on Wyllie's time average) to predict the properties of marine sediments with gas hydrates. Such models give an illusion of being physics-based and thus amenable to generalization. In fact, they cannot be generalized because they are statistical site-specific approximations fine-tuned (by changing the "free" parameters) to a data set selected. The problem with using such models is that they do not provide any rational basis for adapting "free" parameters to conditions at a site that is different from that used for fine-tuning.

Therefore, there is an obvious need for a rational theoretical model to describe the elastic properties of marine sediments. Such a model will allow us to link velocity to porosity in a way consistent with site-specific geologic settings.

MODEL DESCRIPTION

We offer a new first-principle-based effective medium model that takes into account the differential pressure, porosity, and mineralogy of the sediment. The main assumption of the model is that the modulus-pressure behavior of high-porosity sediment is similar to that of a dense random pack of identical elastic spheres. The porosity of this pack is 36 - 40%. In order to extend the model into the high-porosity domain, we use a modification of the Hashin-Shtrikman (1963) upper bound. The model has been described in detail in Dvorkin et al. (1999). Here we summarize the equations needed for a practical application of the model.

First we model the elastic moduli of the dry sediment frame. For porosity ϕ that is smaller than the porosity of the sphere pack ϕ_c, the dry-frame bulk (K_{Dry}) and shear

(G_{Dry}) moduli are:

$$K_{Dry} = [\frac{\phi / \phi_c}{K_{HM} + \frac{4}{3} G_{HM}} + \frac{1 - \phi / \phi_c}{K + \frac{4}{3} G_{HM}}]^{-1} - \frac{4}{3} G_{HM},$$
$$G_{Dry} = [\frac{\phi / \phi_c}{G_{HM} + Z} + \frac{1 - \phi / \phi_c}{G + Z}]^{-1} - Z, \quad Z = \frac{G_{HM}}{6}\left(\frac{9K_{HM} + 8G_{HM}}{K_{HM} + 2G_{HM}}\right), \tag{1}$$

where

$$K_{HM} = [\frac{n^2(1-\phi_c)^2 G^2}{18\pi^2(1-\nu)^2} P]^{\frac{1}{3}}, \quad G_{HM} = \frac{5 - 4\nu}{5(2-\nu)} [\frac{3n^2(1-\phi_c)^2 G^2}{2\pi^2(1-\nu)^2} P]^{\frac{1}{3}}, \tag{2}$$

P is the differential pressure; K, G, and ν are the bulk and shear moduli of the solid phase, and its Poisson's ratio, respectively; n is the average number of contacts per grain in the sphere pack. This number is between 7 and 9 (Mavko et al., 1998).

The differential pressure is the difference between the lithostatic and hydrostatic pressures: $P = (\rho_b - \rho_w) g D$, where ρ_b is the bulk density of the sediment; ρ_w is water density; g is the gravity acceleration; and D is depth below sea floor.

The elastic constants of the solid phase are calculated from those of the individual mineral constituents using Hill's (1952) average formula:

$$K = \frac{1}{2}[\sum_{i=1}^{m} f_i K_i + (\sum_{i=1}^{m} f_i / K_i)^{-1}], \quad G = \frac{1}{2}[\sum_{i=1}^{m} f_i G_i + (\sum_{i=1}^{m} f_i / G_i)^{-1}]; \tag{3}$$

where m is the number of mineral constituents; f_i is the volumetric fraction of the i-th constituent in the solid phase; and K_i and G_i are the bulk and shear moduli of the i-th constituent, respectively.

For porosity that is larger than the porosity of the sphere pack, we have

$$K_{Dry} = [\frac{(1-\phi)/(1-\phi_c)}{K_{HM} + \frac{4}{3} G_{HM}} + \frac{(\phi - \phi_c)/(1-\phi_c)}{\frac{4}{3} G_{HM}}]^{-1} - \frac{4}{3} G_{HM},$$
$$G_{Dry} = [\frac{(1-\phi)/(1-\phi_c)}{G_{HM} + Z} + \frac{(\phi - \phi_c)/(1-\phi_c)}{Z}]^{-1} - Z, \tag{4}$$
$$Z = \frac{G_{HM}}{6}\left(\frac{9K_{HM} + 8G_{HM}}{K_{HM} + 2G_{HM}}\right).$$

For the sediment saturated with pore fluid of bulk modulus K_f, the shear modulus G_{Sat} is the same as that of the dry frame ($G_{Sat} = G_{Dry}$) and the bulk modulus K_{Sat} is calculated from Gassmann's (1951) equation as

$$K_{Sat} = K\frac{\phi K_{Dry} - (1+\phi)K_f K_{Dry} / K + K_f}{(1-\phi)K_f + \phi K - K_f K_{Dry} / K}. \quad (5)$$

The elastic wave velocities are:

$$V_p = \sqrt{(K_{Sat} + \tfrac{4}{3} G_{Sat}) / \rho_B}, \quad V_s = \sqrt{G_{Sat} / \rho_B}; \quad (6)$$

where ρ_B is bulk density. The details of the model are given in Appendix. Porosity used in this model is the total porosity of sediment.

APPLYING NEW MODEL

We apply the new model to six ODP wells worldwide. All these wells penetrate submarine fan channel deposits consisting mainly of turbidites (clay and sand). The locations, water depths, and logged interval extension are given in Table 1.

Table 1. Wells used in the study.

Well Site and Name	Location	Water Depth (m)	Logged Interval (mbsf)
Leg 155, Well 940A	Amazon Delta: Middle Fan	3191	75 – 233
Leg 155, Well 931B	Amazon Delta: Bottom Levee	3476	72 – 251
Leg 155, Well 933A	Amazon Delta: Bottom Levee	3366	69 – 245
Leg 155, Well 946A	Amazon Delta: Middle-to-Lower Fan	4100	78 – 274
Leg 112, Well 679E	Peru Continental Margin	4500	73 – 341
Leg 116, Well 719B	Bengal Distal Fan	4737	87 – 466

Consider first Well 940 located offshore Amazon delta in the Atlantic (Shipboard Scientific Party, 1995). The well log curves for this well are shown in Figure 1. Strong mismatch is apparent between the neutron porosity values and the density-porosity calculated from the bulk density data assuming that the density of the pore fluid is 1 g/cm^3 and that of the mineral phase is 2.65 g/cm^3 (Figure 1c). The neutron porosity values are likely to overestimate the total porosity in a clay-rich environment (Wetzel et al., 1990) because of large amount of bound water in clay minerals. As a result, we use

the calculated density-porosity curve as the total porosity input for our modeling.

The bulk modulus of sea water used in our modeling is 2.46 GPa and its density is 1.038 g/cm^3. These values correspond to 32 – 34 MPa pressure (sea depth below 3000 m) and 3 – 10 °C temperature (Batzle and Wang, 1992). Flood et al. (1997) estimate that the main mineralogical components of the sediment in this well are clay and quartz, with clay content between 60% and 80%. Accordingly, we assumed that the sediment's mineralogy only included quartz and clay with uniform (70%) clay content. The corresponding bulk and shear moduli of the mineral phase of the sediment, according to Equation (3) were 25 GPa and 14 GPa, respectively. These values are summarized in Table 2. Pure mineral properties are taken from Mavko et al. (1998).

Table 2. Material properties.

Material	Density (g/cc)	Bulk Modulus (GPa)	Shear Modulus (GPa)
Quartz	2.65	36.6	45
Clay	2.54	21	7
Sea Water	1.038	2.46	0
30% Quartz + 70% Clay	2.60	25	14
85% Quartz + 15% Clay	2.64	33.6	31.9

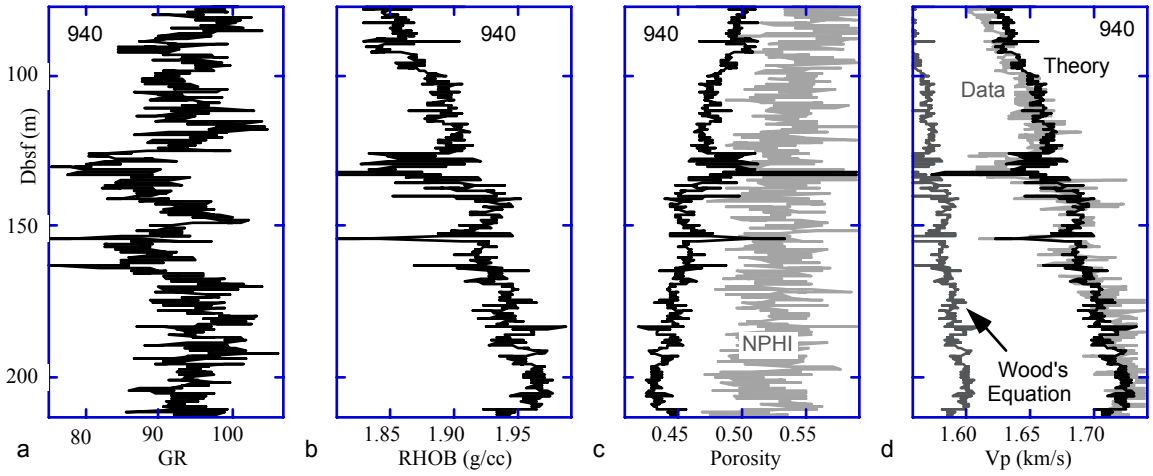

Figure 1. Well log curves for ODP well 940 (Shipboard Scientific Party, 1995). (a) Gamma-ray; (b) bulk density; (c) density-porosity (black) and neutron porosity (gray); (d) P-wave velocity data (gray) and modeled values (black). Wood's equation (1941) prediction that grossly underestimates measured velocity is plotted in "d" for comparison.

The calculated theoretical velocity values accurately match the data (Figure 1d).

The modeled velocity, together with the measured velocity, is plotted versus the density-porosity in Figure 2a. The relative mismatch between the theoretical velocity values and the data is plotted versus depth in Figure 2b. This mismatch is small and does not exceed 2%.

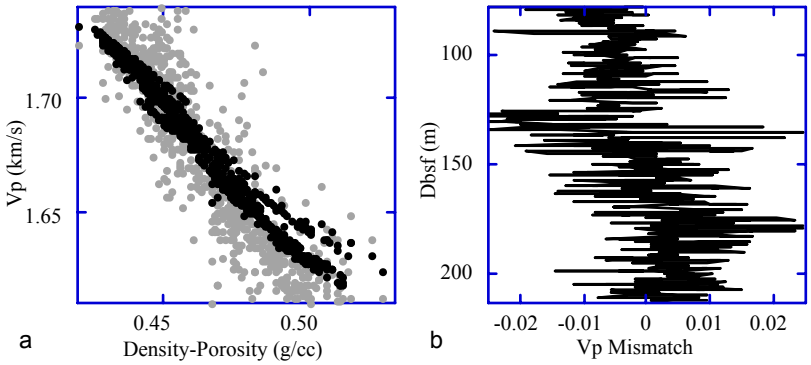

Figure 2. ODP well 940. (a) P-wave velocity data (gray) and modeled values (black) versus density-porosity; (b) relative mismatch between velocity data and modeled velocity versus depth.

Our next example is Well 931 (Figure 3) that is in the same location as Well 940 (Shipboard Scientific Party, 1995). The modeling input parameters are the same as in the previous example. The results of velocity modeling are compared to the velocity data in Figure 3d. The theoretical values calculated using the density-porosity as input closely match the data.

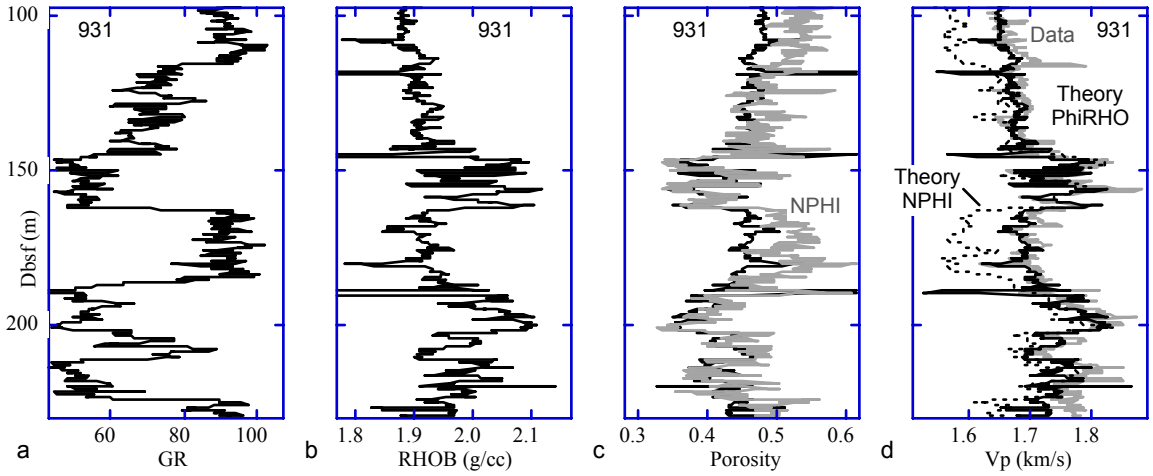

Figure 3. Well log curves for ODP well 931 (Shipboard Scientific Party, 1995). (a) Gamma-ray; (b) bulk density; (c) density-porosity (black) and neutron porosity (gray); (d) P-wave velocity data (gray) and modeled values (black). The dashed line is theoretical velocity calculated with neutron porosity as input.

Other two wells from the same location used for modeling are Well 933 (Figure 4) and Well 946A (Figure 5) (Shipboard Scientific Party, 1995). The modeling parameters and mineralogy are the same as used in the first example. The theoretical-model velocity values closely match the data practically in the entire depth range. Again, it was essential to use the density-porosity rather than neutron porosity as an input.

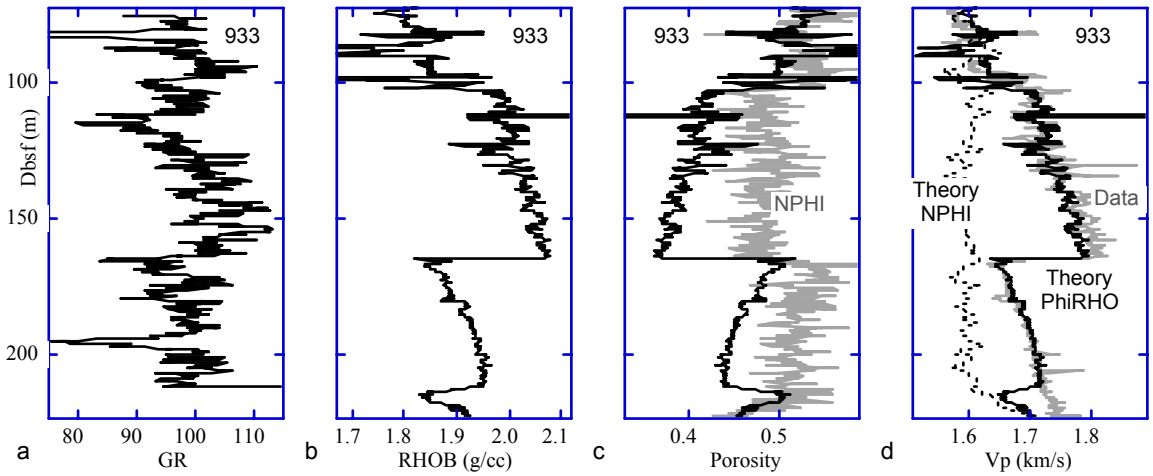

Figure 4. Well log curves for ODP well 933 (Shipboard Scientific Party, 1995). (a) Gamma-ray; (b) bulk density; (c) density-porosity (black) and neutron porosity (gray); (d) P-wave velocity data (gray) and modeled values (black). The dashed line is theoretical velocity calculated with neutron porosity as input.

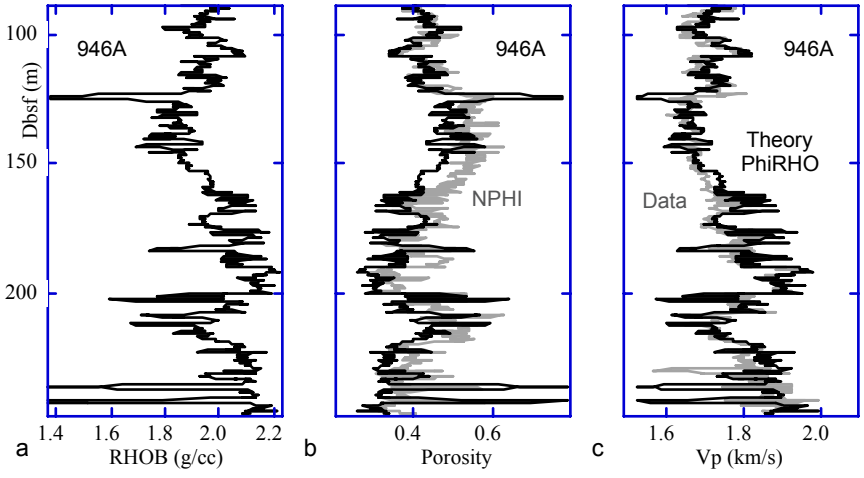

Figure 5. Well log curves for ODP well 946A. (a) Bulk density; (b) density-porosity (black) and neutron porosity (gray); (c) P-wave velocity data (gray) and modeled values (black).

A lithological boundary present in Well 933 at 164 mbsf changes the character of well log curves (Figure 4b, c, and d) but does not affect the applicability of our

theoretical model. The reason is that the texture and mineralogy of the sediment does not change as it progresses from debris-flow deposit to deep levee deposit at about 164 mbsf (Flood et al., 1998).

The match between the theoretical values and the data is accurate in the entire interval, except the very bottom portion (214 mbsf) where the modeled velocity is smaller than the measured velocity. This may be due to textural changes in the sediment or poor quality of the data in the very bottom portion of the logged interval.

Our next example is ODP Well 679E in Peru Margin (Figure 6) (Shipboard Scientific Party, 1988). The interval is characterized as siliceous ooze and mudstone with some siltstone (Anderson and Greenberg, 1990). The input parameters used are the same as in the previous examples. The match between the modeled velocity and the data is good in the entire interval except the very bottom part below 255 mbsf.

In this bottom interval, the theoretical model under-predicts the data. This is likely to be the result of texture change and diagenesis in the sediment. Indeed, the lithology changes into mudstone and dolomite at 255 mbsf with indications of calcite cementation (Shipboard Scientific Party, 1988). The unconsolidated marine sediment model offered in this paper is not applicable to the sediment where diagenetic cementation may have taken place.

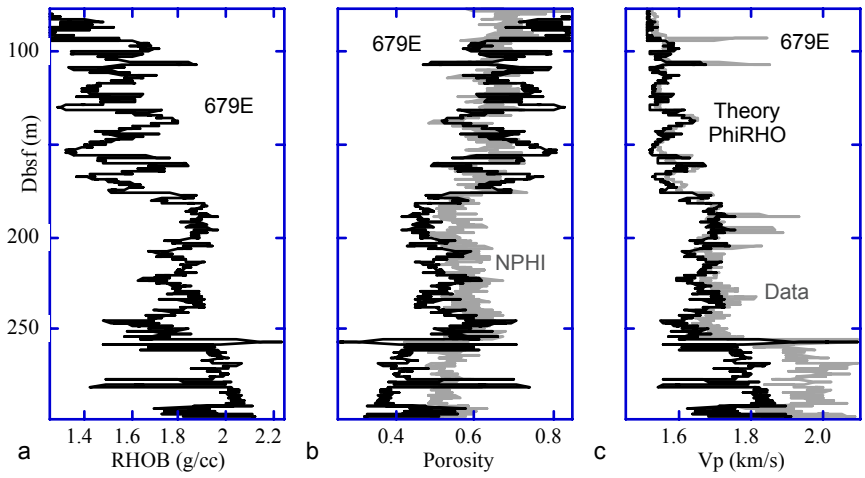

Figure 6. Well log curves for ODP well 679E (Shipboard Scientific Party, 1988). (a) Bulk density; (b) density-porosity (black) and neutron porosity (gray); (c) P-wave velocity data (gray) and modeled values (black).

Our final example is for ODP Well 719B (Figure 7) in the Bengal Bay (Shipboard Scientific Party, 1989). In this example, in order to match the velocity data, we had to assume that the mineralogy of the sediment is 85% quartz and 15% clay. As a result, we achieve consistent match between the theoretical velocity values and the data in the entire depth interval (Figure 7c).

This selection of mineralogy, although seemingly arbitrary, is consistent with the description of the core from this well (Cochran, 1990). The entire sequence consists of turbidite silt-rich deposits with thin interbedded pelagic clays. Therefore, it appears that the sediment at this Bengal Bay location is predominantly quartz. This fact is also consistent with a good match between the neutron porosity and density-derived porosity in the interval (Figure 7b).

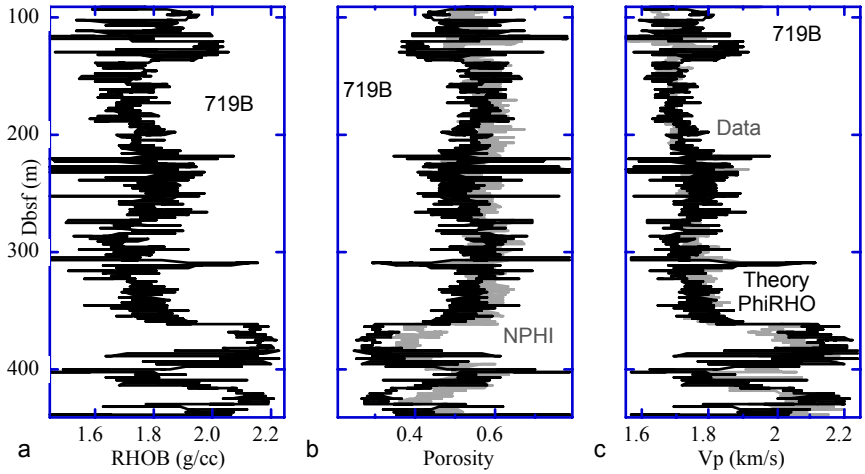

Figure 7. Well log curves for ODP well 719B (Shipboard Scientific Party, 1989). (a) Bulk density; (b) density-porosity (black) and neutron porosity (gray); (c) P-wave velocity data (gray) and modeled values (black).

CONCLUSION

Our new theoretical model allows to consistently match well log velocity data using porosity as the main input. This modeling is accurate only if the mineralogy of the sediment is properly calibrated to the site-specific conditions. This model is intended to be used as an alternative to traditional velocity-porosity transforms in log analysis and interpretation. The model can only be applied to unconsolidated marine sediment and should not be used for cemented and diagenetically altered rock.

ACKNOWLEDGMENTS

This work was supported by the Stanford Rock Physics Laboratory.

APPENDIX: EFFECTIVE MEDIUM MODEL

To relate the elastic moduli of sediment to porosity, pore fluid compressibility, mineralogy, and differential pressure, we first model the elastic moduli of the dry rock frame.

Porosity Below Critical (Dvorkin and Nur, 1996). For unconsolidated rock whose porosity is below critical ϕ_c (ϕ_c = 36 - 40%, Nur et al., 1998), this effective medium model connects two end points in the modulus-porosity plane, one at zero porosity where the rock's elastic moduli are those of the solid phase (Figure A1a), and the other at ϕ_c where sediment is modeled as a random pack of identical spheres (Figure A1c).

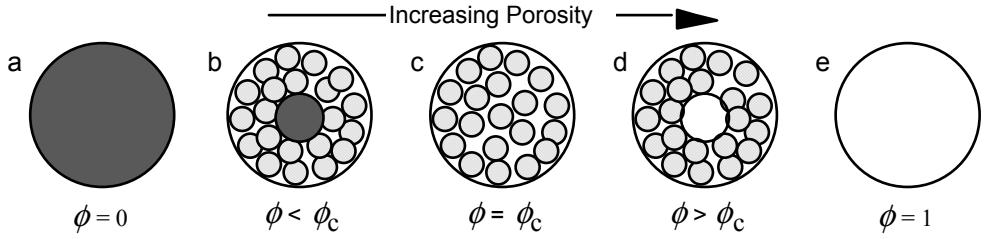

Figure A1. Hashin-Shtrikman arrangements of sphere pack, solid, and void. From left to right: pure solid at zero porosity; pure solid enveloped by the sphere pack phase; sphere pack at critical porosity; void enveloped by sphere pack phase; and void at 100% porosity.

At zero porosity, the bulk and shear moduli of the rock are those of the solid phase (K and G, respectively). At ϕ_c, the effective bulk (K_{HM}) and shear (G_{HM}) moduli of this pack (dry) are given by the Hertz-Mindlin equation (2) – see main text.

These two end points in the porosity-moduli plane can be connected with the curves that have algebraic expressions of the upper or lower Hashin-Shtrikman (1963) bound (bulk and shear moduli) for the mixture of two components: the pure solid phase and the phase that is the sphere pack. The lower bound is most appropriate because we are modeling unconsolidated sediment and, therefore, looking for the softest arrangement of

the two end-point materials. A physical realization of this arrangement (but not necessarily a real sediment texture) shown in Figure A1b is that the softest component (the sphere pack) envelopes the stiffest component (the solid).

To mathematically express this lower bound, we notice that at porosity ϕ the concentration of the pure solid phase in the rock is $1-\phi/\phi_c$ and that of the sphere-pack phase is ϕ/ϕ_c. Then the bulk (K_{Dry}) and shear (G_{Dry}) moduli of the dry frame are given by Equation (1) in the main text.

Porosity Above Critical. For high-porosity marine sediment, the low-porosity end point is at ϕ_c (Figure A1c) and the elastic moduli come from hertz-Mindlin equations (2) in the main text. Marine sediment is unlikely to look like a pack of identical spheres. The role of this pack is only to provide the end-point elastic moduli for building the desired effective-medium model. The other end point (Figure A1e) at 100% porosity is (without pore fluid) void of zero rigidity. As in the below-critical-porosity case, consider two elastic bounds for the dry frame. The lower one, where the softest component (voids of zero rigidity) dominates, has zero elastic moduli. The upper one (Figure A1d) has a physical realization (not to be confused with the actual sediment texture) where the stiffest component (the sphere pack) is placed around the softest component (the void). Our intention is to model sediment with a non-zero stiffness of the dry frame. This is why we hypothesize that the appropriate elastic moduli come from the upper Hashin-Shtrikman bound.

At porosity $\phi > \phi_c$, the concentration of the void phase is $(\phi-\phi_c)/(1-\phi_c)$ and that of the sphere-pack phase is $(1-\phi)/(1-\phi_c)$. Then the effective dry-frame moduli are given by Equation (4) in the main text.

REFERENCES

Anderson, R. N. and Greenberg, M. L., 1990, Composition of sediments from the Peru upwelling area: Results from sites 680, 682, 685, and 688. *In* Suess, E., von Huene, R., et al., 1990, *Proc. ODP, Sci. Results*, 112: College Station, TX (Ocean Drilling Program), 481-490.

Batzle, M., and Wang, Z., Seismic properties of pore fluids, Geophysics, 57, 1396-1408, 1992.

Cochran, J. R., 1990, Himalayan uplift, sea level, and the record of Bengal Fan sedimentation at the ODP Leg 116 sites. *In* Cochran, J. R., Stow, D. A. V., et al., 1990, *Proc. ODP, Sci. Results*, 116: College Station, TX (Ocean Drilling Program), 397-414.

Dvorkin, J., and Nur, A., 1998, Time-Average Equation Revisited, Geophysics, 63, 460-464.

Dvorkin, J., Prasad, M., Sakai, A., and Lavoie, D., 1999, Elasticity of marine sediments, Geophysical Research Letters, 26, 1781-1784.

Flood, R. D., Primez, C., Yin, H., 1997, The compressional-wave velocity of Amazon Fan sediments: Calculations from index properties and variations with clay content. *In* Flood, R. D., Piper, D. J. W., Klaus, A., Petersen, L. C., (Eds.), *Proc. ODP, Sci. Results*, 155: College Station, TX (Ocean Drilling Program), 477-493.

Gassmann, F., Elasticity of porous media: Uber die elastizitat poroser medien: Vierteljahrsschrift der Naturforschenden Gesselschaft, 96, 1-23, 1951.

Hamilton, E.L., Elastic properties of marine sediments, JGR, 76, 579-604, 1971.

Hamilton, E.L., Shear-wave velocity versus depth in marine sediments: A review, Geophysics, 41, 985-996, 1976.

Hashin, Z., and Shtrikman, S., A variational approach to the elastic behavior of multiphase materials, J. Mech. Phys. Solids, 11, 127-140, 1963.

Hill, R., The elastic behavior of crystalline aggregate, Proc. Physical Soc., London, A65, 349-354, 1952.

Lee, M.W., Hutchinson, D.R., Collet, T.S., and Dillon, W.P., Seismic velocities for

hydrate-bearing sediments using weighted equation, JGR, 101, 20,347-20,358, 1996.

Mavko, G., Mukerji, T., and Dvorkin, J., The rock physics handbook, Cambridge University Press, 1998.

Nobes, D.C., Villinger, H., Davis, E.E., and Law, L.K., Estimation of marine sediment bulk physical properties at depth from seafloor geophysical measurements, JGR, 91, 14,033-14,043, 1986.

Reuss, A., Berechnung der Fliessgrenzev von Mischkristallen auf Grund der Plastizitätsbedingung für Einkristalle, Zeitschrift für Angewandte Mathematik und Mechanik, 9, 49-58, 1929.

Richardson, M.D., and Briggs, K.B., On the use of acoustic impedance values to determine sediment properties, Proceedings of the Institute of Acoustics, 15, 15-23, 1993.

Shipboard Scientific Party, 1988, Site 719: Bengal Fan. *In* Cochran, J. R., Stow, D. A. V., et al., 1988, *Proc. ODP, Init. Repts.*, 116: College Station, TX (Ocean Drilling Program), 347-380.

Shipboard Scientific Party, 1989, Site 679. *In* Suess, E., von Huene, R., et al., 1990, *Proc. ODP, Init. Repts.*, 112: College Station, TX (Ocean Drilling Program), 159-248.

Shipboard Scientific Party, 1995, Sites 931-946. *In* Flood, R. D., Piper, D. J. W., Klaus, A., Petersen, L. C., (Eds.), *Proc. ODP, Init. Repts.*, 155: College Station, TX (Ocean Drilling Program), 123-696.

Wetzel, A., Williams, C., Kassens, H., Leger, G., Auroux, C., 1990, Comparison between laboratory-determined physical properties and downhole measurements in outer Bengal Fan deposits. *In* Cochran, J. R., Stow, D. A. V., et al., 1990, *Proc. ODP, Sci. Results*, 116: College Station, TX (Ocean Drilling Program), 369-374.

Wilkens, R.H., Cheng, C.H., and Meredith, J.A., Evaluation and prediction of shear wave velocities in calcareous marine sediment and rocks, JGR, 97, 9,297-9,305, 1992.

Wood, A.B., A textbook of sound, G. Bell and Sons, Ltd., London, 1941.

Wyllie, M.R.J., Gregory, A.R., and Gardner, L.W., Elastic wave velocities in heterogeneous and porous media, Geophysics, 21, 41-70, 1956.